Supplementary Online Information

$Revision$: 1.5, June 10, 2005

Carbonate chemistry

We computed [CO_3^{2-}] and other carbonate system variables using the standard OCMIP carbonate chemistry routines. The equilibrium constants K_1 and K_2 are those from Mehrbach et al.[1] refit to the total pH scale[2]; K_B, K_{1P}, K_{2P}, K_{3P}, K_{Si} and K_W are from Millero[3]; K_S is from Dickson[4]; and K_F is from Dickson and Riley[5]. These are apparent equilibrium constants, given in terms of concentrations, not activities. Constants are referenced to the total pH scale, except for K_S, which is on the free pH scale. To calculate saturation, we used the apparent solubility products for aragonite Ksp_A^* and calcite Ksp_C^* from Mucci[6]. For magnesian calcite, some forms can be more soluble than aragonite [6,7]. We accounted for pressure-related changes in these equilibrium constants using the formulations of Millero[3]. The uncertainty in the computation of [CO_3^{2-}] from modelled DIC and alkalinity is $<\pm 1$ μmol kg^{-1} based on our sensitivity tests with the other currently accepted sets of constants and pH scales.

To compute the level of saturation with respect to $CaCO_3$, we used the standard definition, $\Omega = [Ca^{2+}][CO_3^{2-}]/[Ksp^*]$, where the apparent solubility product Ksp^* is different for aragonite (A) and calcite (C). Because variations in Ω are essentially due to [CO_3^{2-}] (i.e., [Ca^{2+}] varies by only a few percent in the open ocean) we also employed a convenient, carbonate-specific index

of saturation $\Delta[CO_3^{2-}] = [CO_3^{2-}] - [CO_3^{2-}]_{sat}$, where $[CO_3^{2-}]_{sat}$ is the $[CO_3^{2-}]$ for seawater in equilibrium with $CaCO_3$ at the in situ temperature and salinity[8] (see Fig. 2). Both terms are used to indicate that a solution is supersaturated ($\Omega > 1$ and $\Delta[CO_3^{2-}] > 0$) or undersaturated ($\Omega < 1$ and $\Delta[CO_3^{2-}] < 0$).

Transient change

We computed the 21st century decline in ocean $[CO_3^{2-}]$ due to ocean uptake of anthropogenic CO_2 using the three-dimensional fields of DIC, alkalinity, temperature, and salinity from 13 models that participated in OCMIP-2. Most of these models include the annual cycle. We discuss annual mean changes to focus on the transient signal from increasing anthropogenic CO_2. These models have been previously evaluated[9–11] and documented in terms of their simulated anthropogenic CO_2 uptake[12–14]. To simplify comparison during OCMIP-2, all models were run under modern, prescribed climate. Thus they did not account for interannual or future changes in climate and alkalinity.

Climate change

To estimate how future climate change will induce shifts in ocean carbonate chemistry, we used output from three physical-biogeochemical climate models: (1) the PIUB-Bern model (Physics Institute at the University of Bern, Switzerland) is a reduced complexity coupled system that includes a zonally averaged ocean model[15], an atmospheric energy balance model[16], and both marine[17] and terrestrial[18] carbon cycle components; (2) the CSIRO (Commonwealth Scientific and Industrial Re-

search Organisation, Australia), is a more complex atmosphere-ocean-ice climate model[19,20] that has been coupled to a simplified prognostic oceanic biogeochemical model[21]; and (3) the IPSL model (Institute Pierre Simon Laplace, France), is also a more complex atmosphere-ocean-ice climate model that is also coupled to both marine and terrestrial carbon cycle components [22].

We estimated future changes in $[CO_3^{2-}]$ due only to changes in climate by running multiple simulations in each model. With the CSIRO model, we used the difference in $[CO_3^{2-}]$ between two simulations: *i)* a transient simulation where future atmospheric CO_2 followed the IS92a scenario, and *ii)* a control simulation where ocean biogeochemistry followed the same atmospheric CO_2 trajectory, but where radiative forcing was computed from an constant atmospheric CO_2 of 330 ppmv. Similarly, with the PIUB-Bern model we used the difference between two simulations where in both cases atmospheric CO_2 was prescribed according to scenario IS92a[23,24]: *i)* a constant climate simulation where the atmospheric CO_2 increase did not affect radiative forcing and *ii)* a climate change simulation where radiative forcing followed the atmospheric CO_2 increase. With the IPSL model, isolating the effect of climate change required three simulations: *i)* a prescribed climate simulation (LF9), where atmospheric CO_2 reached 695 ppmv in 2100; *ii)* a changing climate simulation with full carbon-climate feedback (LF8), where atmospheric pCO_2 reached 780 ppmv in 2100; and *iii)* a combined simulation (LFB), which was forced with the atmospheric CO_2 from LF9 but the climate from LF8. For IPSL, we present differences in ocean $[CO_3^{2-}]$ between LFB and LF9, which are driven only by changes in ocean circulation.

Climate variability

For the interannual simulation, we used the ORCA2 global configuration of the Ocean Parallelisé (OPA) ocean general circulation model[25], version 8.1, that was forced with the NCEP reanalysis from 1948–2003 as described by Rodgers et al.[26]. This circulation model was coupled to the biogeochemical model known as PISCES[27,28], which includes the OCMIP carbon chemistry as well as micronutrient limitation and two classes each of phytoplankton, zooplankton, and detritus.

Potential change in respiration

Biological respiration of organic matter produces DIC and thus reduces $[CO_3^{2-}]$. Although much research has focused on quantifying respiration rates, little is known about how much these rates might be changing on decadal time scales[29]. In the surface ocean, observed decadal changes in dissolved O_2 and apparent oxygen utilisation (AOU) may be caused by changes in biological productivity and respiration as well as changes in circulation; however, distinguishing which factor is most important remains difficult[30]. For surface $[CO_3^{2-}]$ though, it matters little whether or not surface organic matter production and respiration change because corresponding changes in surface DIC will largely be compensated by air-sea CO_2 exchange. Furthermore, future scenarios with coupled climate-carbon models suggest that DIC changes from changes in circulation are oftern opposite to those due to changes in production, with circulation generally dominating[31,32]. In short, for the surface ocean, where the changes in $[CO_3^{2-}]$ and the corresponding biological impacts will be largest, the dominant control will be the anthropogenic CO_2 invasion.

In contrast, for deeper waters, e.g., near today's aragonite saturation horizon, such compensation is lacking. Changes in DIC due to changes in respiration would thus have a larger impact. In those waters, recent respiration-driven changes in DIC could perhaps rival current anthropogenic DIC concentrations ($<$10 μmol kg^{-1}, Fig. S4). But as we move further into the 21st century, the invasion of anthropogenic CO_2 will rapidly overwhelm the system. Anthropogenic DIC will generally reach 100 μmol kg^{-1} or more near the aragonite saturation horizon in 2100 (Fig. S5). For comparison, coupled climate-carbon models[24,31,33,34] simulate changes in dissolved O_2 in the thermocline that are less than a few tens of μmol kg^{-1} for basin-wide averages in 2100. If these changes in O_2 were due purely to respiration of organic matter, the corresponding change in [CO_3^{2-}] would be of similar magnitude (based on $\Delta\text{DIC}_{resp} = r\text{C:O}_2 \times \Delta\text{AOU}$, where $r\text{C:O}_2 \approx 1.4$[35]). Yet these changes in O_2 in the coupled climate-carbon models result essentially from changes in circulation; changes in respiration are small. Furthermore, the most recent studies that have looked carefully at observed decadal changes of O_2 in the thermocline find that they may be largely explained by changes in circulation without need to invoke changes in biological respiration[36,37].

Although the three coupled climate-carbon models used in this study do account for changes in new production and respiration, by definition their accounting is simplified. For instance, global ocean carbon cycle models are just beginning to account for how changes in [CO_3^{2-}] might affect biological export and remineralisation[38]. Models may over- or under-estimate the extent to which subsurface [CO_3^{2-}] will change due to climate-driven changes in respiration. However, we argue in the main text that the simulated trend is robust: changes in respiration only further reduce high-latitude subsurface [CO_3^{2-}]. That trend is consistent with a more active hydrological cycle in a

future warmer world, as predicted by all climate models.

Potential change in alkalinity

Future changes in alkalinity due to dissolution of carbonate material in shallow- and deep-ocean sediments should be negligible for a 100-year timescale[39,40]. However, Sarma et al.[41] recently suggested that alkalinity increased between the 1970's and the 1990s at the depth of the aragonite saturation horizon in the Pacific and Indian Oceans. At their two repeat stations in the subarctic Pacific, occupied during the GEOSECS and WOCE campaigns, alkalinity increased by 13 ± 6 and 11 ± 6 μmol kg^{-1}. Yet there was not only a change in alkalinity; DIC also increased by about 1.5 times as much (21 ± 7 and 16 ± 7 μmol kg^{-1}). At the station with the largest WOCE $-$ GEOSECS changes in DIC and alkalinity, we calculate that the corresponding decline in [CO_3^{2-}] is -3.5 ± 9 μmol kg^{-1}. On the other hand, the computed decline in [CO_3^{2-}] would be larger (-5.2 μmol kg^{-1}) had we taken the simplified approach, i.e., neglecting alkalinity changes and accounting only for the corresponding 11 μmol kg^{-1} anthropogenic DIC increase. The latter was estimated by Sarma et al. by correcting for increases in DIC and alkalinity due to increases in AOU and $CaCO_3$ dissolution

$$CO_2 + CaCO_3 + H_2O \rightarrow 2HCO_3^- + 2Ca^{2+}.$$

Unfortunately, the large $\pm 1\sigma$ uncertainties do not permit us to distinguish if there have been significant changes in [CO_3^{2-}] due to enhanced $CaCO_3$ dissolution between GEOSECS and WOCE. Future studies will be in a better position to resolve this question because the signal is growing exponentially and the precision of DIC and alkalinity measurements has improved greatly since GEOSECS. Although our simplified approach may overestimate the decline in future [CO_3^{2-}] at

the saturation horizon, such may be compensated by opposite trends elsewhere, as suggested by simultaneous reductions in alkalinity just above and below the same horizon (Fig. 3 of Sarma et al.).

Supplementary Online Table

Table S1: Area-weighted mean depth (m) of the aragonite saturation horizon.

Time	Southern Ocean ($< 60°$S)	North Atlantic (50°N–70°N)	North Pacific (50°N–60°N)	Global
Preindustrial (data-based)	1038	2825	177	1089
1994 (GLODAP)	727	2602	142	959
2100 (S650)	*59	612	74	*425
2100 (IS92a)	*2	116	*40	*277

* Before averaging, the depth was set to 0 m in grid cells where surface $\Omega_A < 1$.

Supplementary Online Figures and Figure Legends

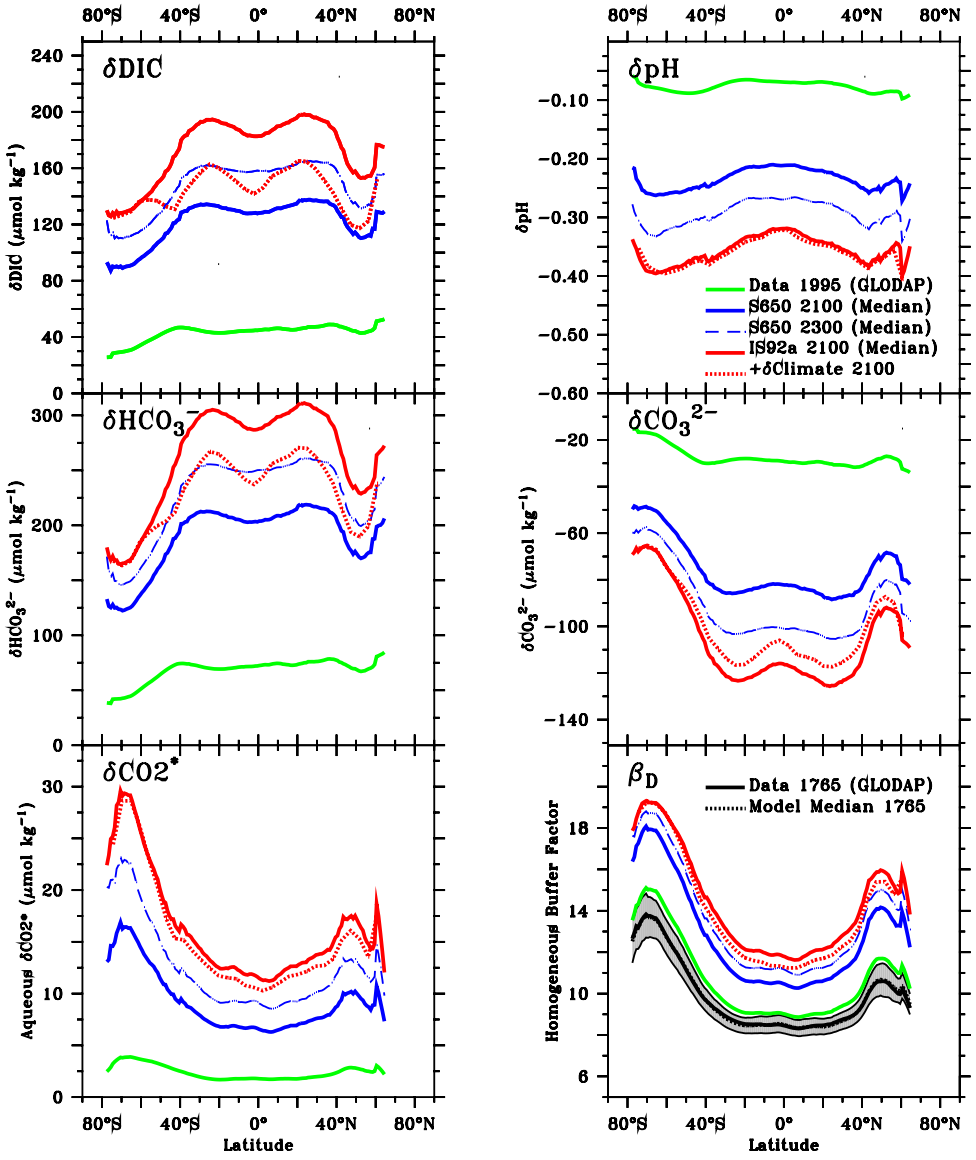

Figure S1 Changes in carbonate chemistry variables relative to the preindustrial ocean: 1994 (green), 2100 from IS92a (red) and S650 (blue), 2300 from S650 (blue dashed). Future climate change from the IPSL model (red dotted line) is shown as a perturbation to IS92a in 2100. Also shown is the homogeneous buffer factor β_D.

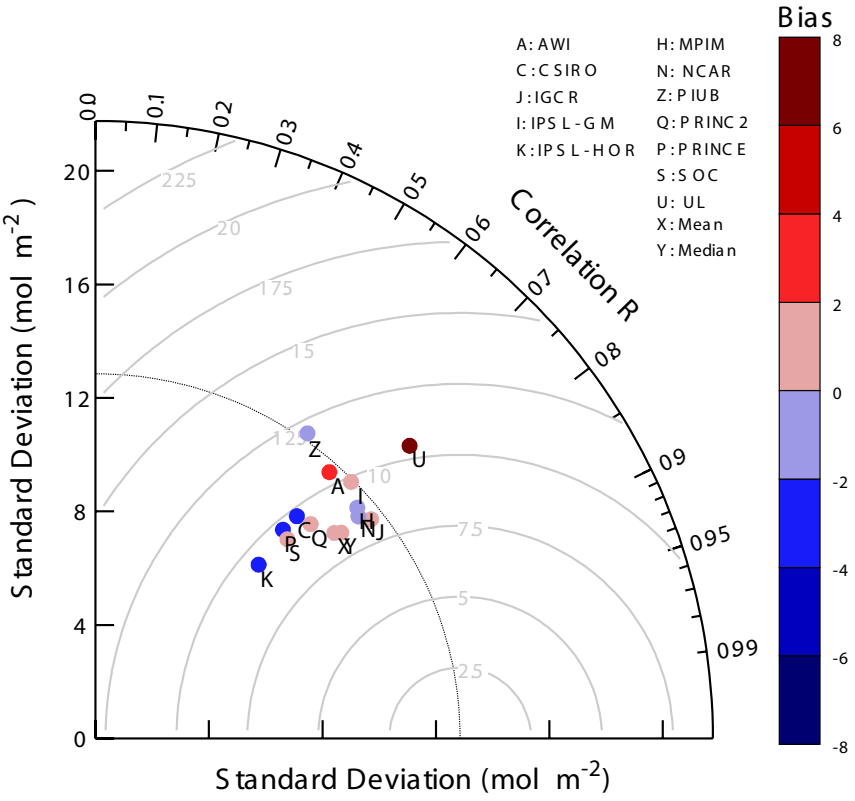

Figure S2 Taylor Diagram[42] for the map of the column integral (inventory) of anthropogenic CO_2 between 50°S and 50°N. A Taylor diagram is a polar plot that compares models to a data reference for 3 summary statistics: (1) the standard deviation σ on the radial axis, (2) the correlation coefficient R on the angular axis, (3) the central pattern r.m.s. error as the distance (radius of semicircles) from the data reference point on the x axis (centre of semi-circles). We have also added a fourth statistic, the overall bias (area weighted mean for the model minus that for the data), as the coloured point whose intensity is indicated by the colour bar. All four statistics are in units of mol m^{-2}. Overall, the median (Y) of the OCMIP-2 models exhibits the greatest skill, i.e., it generally lies closer to the data reference[43] than do the individual models.

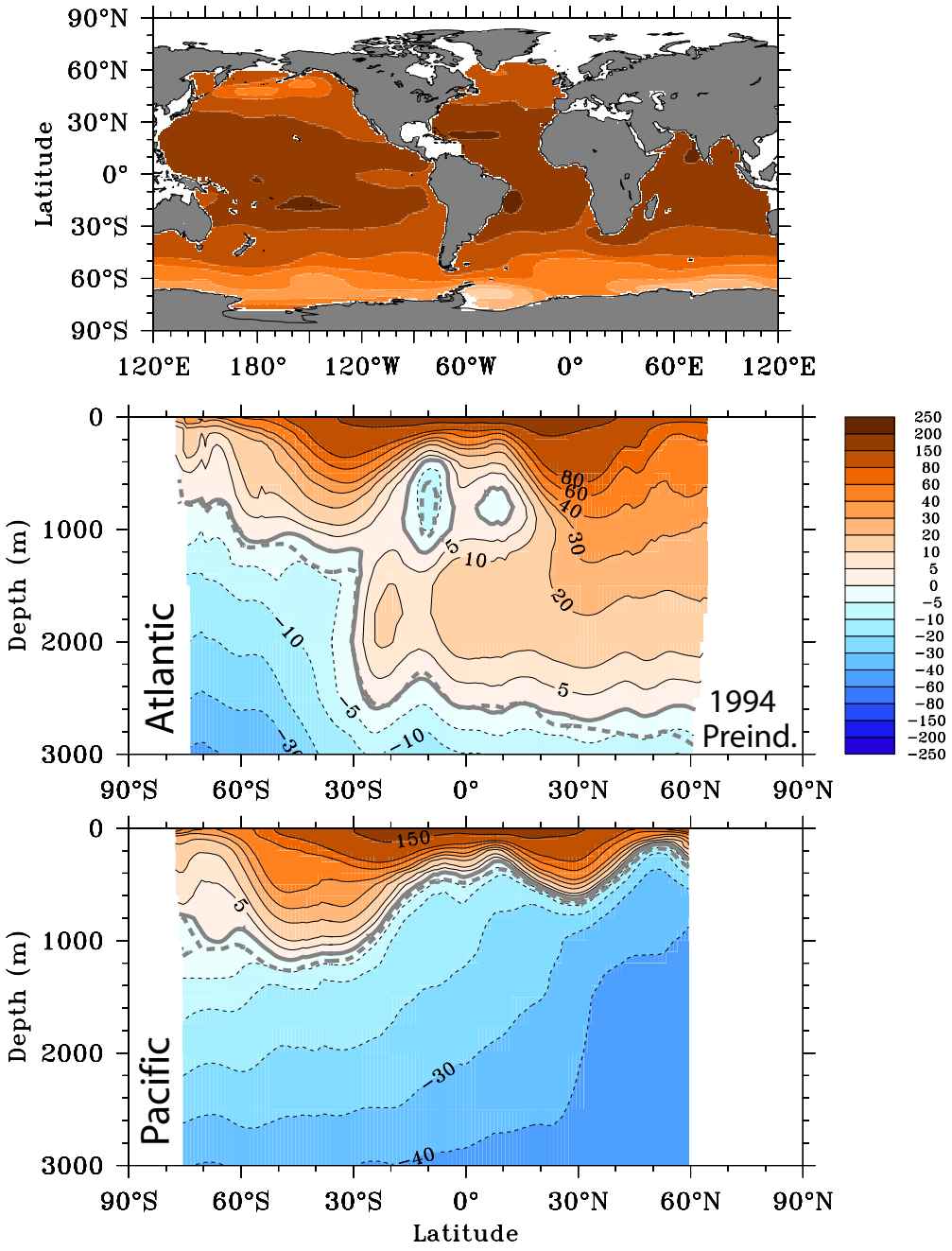

Figure S3 Excess carbonate concentration $\Delta[CO_3^{2-}]_A$ in 1994 for comparison with Fig. 2. Lines correspond with the aragonite saturation horizon ($\Omega_A = 1$) in 1765 (dashed grey) and 1994 (solid grey).

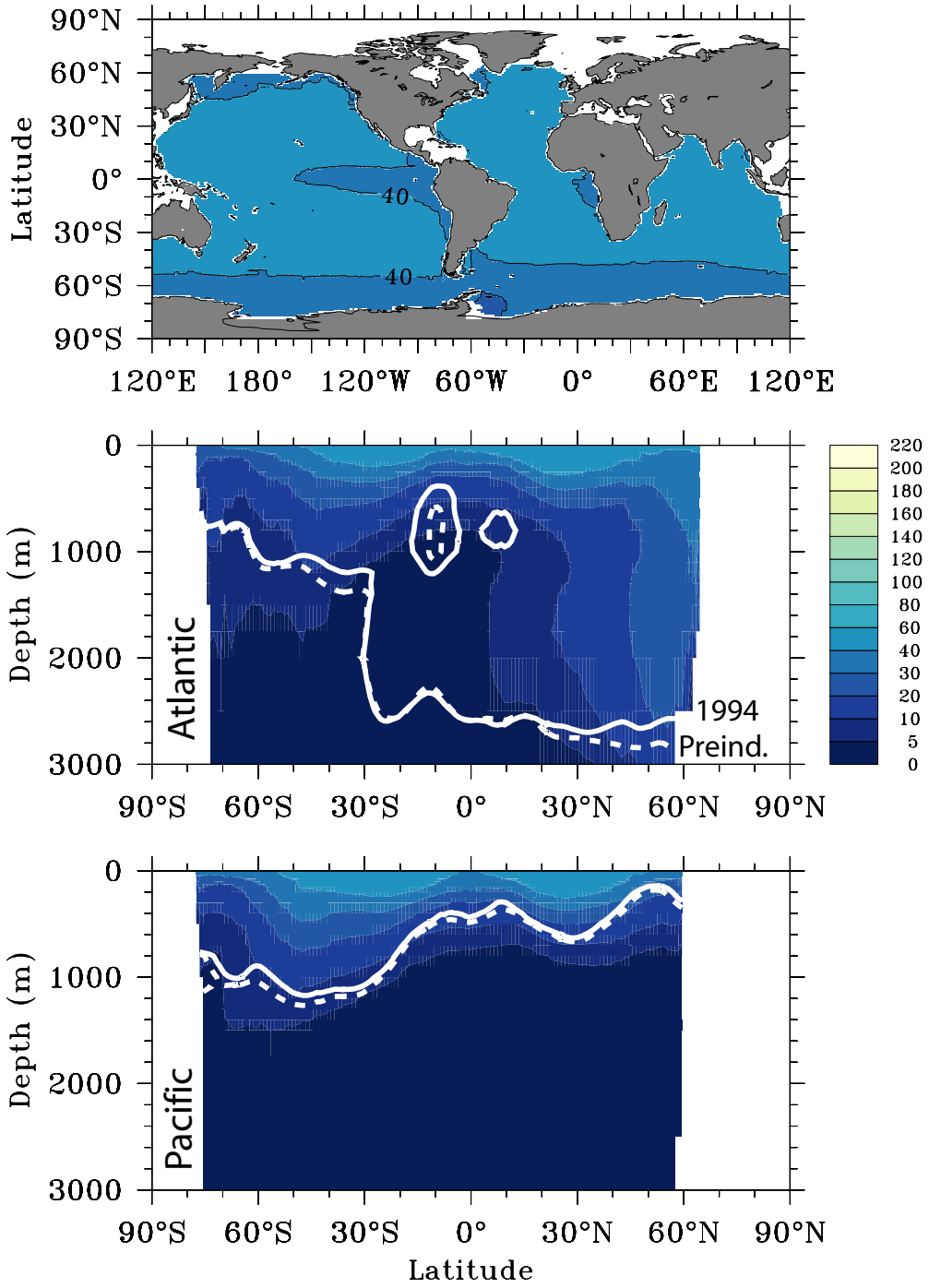

Figure S4 Median anthropogenic DIC in 1994 from the OCMIP-2 models. Lines are given for the aragonite saturation horizon in the preindustrial ocean (white dashed) and in 1994 (white solid), as in Fig. S3.

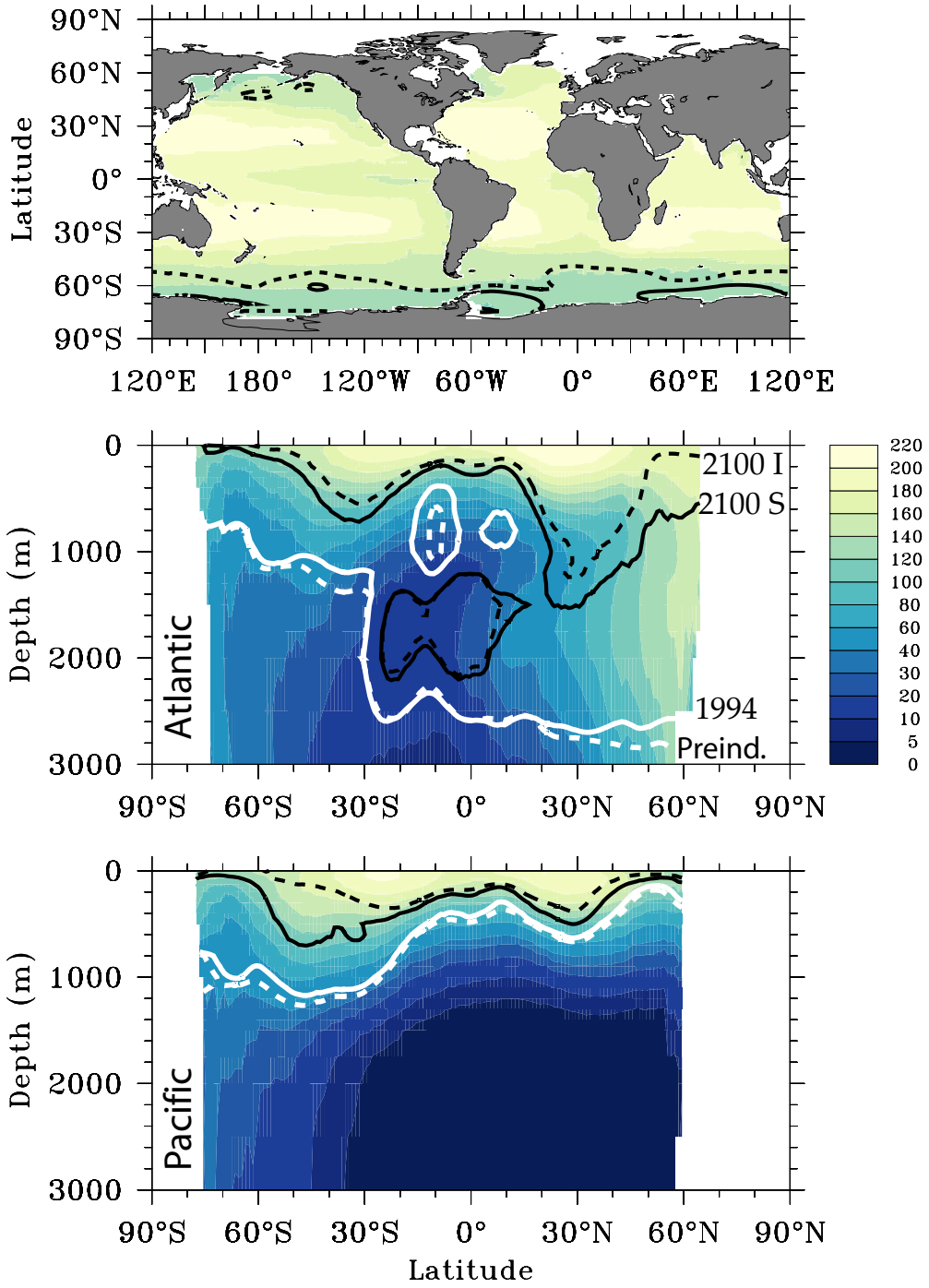

Figure S5 Median anthropogenic DIC in 2100 from the OCMIP-2 models under the IS92a scenario. The aragonite saturation horizon is also given for 2100 under both the S650 (2100 S, black solid) and IS92a (2100 I, black dashed) scenarios.

Supplementary Online References

1. Mehrbach, C., Culberson, C. H., Hawley, J. E. & Pytkowicz, R. M. Measurement of the apparent dissociation constants of carbonic acid in seawater at atmospheric pressure. *Limnol. Oceanogr.* **18**, 897–907 (1973).

2. Lueker, T. J., Dickson, A. G. & Keeling, C. D. Ocean pCO_2 calculated from dissolved inorganic carbon, alkalinity, and equations for K_1 and K_2: validation based on laboratory measurements of CO_2 in gas and seawater at equilibrium. *Mar. Chem.* **70**, 105–119 (2000).

3. Millero, F. J. Thermodynamics of the carbon dioxide system in the oceans. *Geochimica et Cosmochimica Acta* **59**, 661–677 (1995).

4. Dickson, A. G. Thermodynamics of the dissociation of boric acid in synthetic seawater from 273.15 to 318.15 K. *Deep-Sea Res.* **37** (1990).

5. Dickson, A. G. & Riley, J. P. The estimation of acid dissociation constants in seawater media from potentiometric titrations with strong base. I. The ionic product of water - Kw. *Mar. Chem.* **7** (1979).

6. Mucci, A. The solubility of calcite and aragonite in seawater at various salinities, temperatures, and one atmosphere total pressure. *Am. J. Sc.* **283**, 780–799 (1983).

7. Bischoff, W. W., Mackenzie, F. T. & Bishop, F. C. Stabilities of synthetic magnesian calcites in aqueous solution: comparison with biogenic materials. *Geochimica et Cosmochimica Acta* **51**, 1413–1423 (1987).

8. Archer, D. An atlas of the distribution of calcium carbonate in sediments of the deep sea. *Global Biogeochem. Cycles* **10**, 159–174 (1996).

9. Dutay, J.-C. *et al.* Evaluation of ocean model ventilation with CFC-11: Comparison of 13 global ocean models. *Ocean Modelling* **4**, 89–120 (2002).

10. Doney, S. *et al.* Evaluating global ocean carbon models: The importance of realistic physics. *Global Biogeochem. Cycles* **18**, GB3017, doi:10.1029/2003GB002150 (2004).

11. Dutay, J.-C. *et al.* Evaluation of OCMIP-2 ocean models' deep circulation with mantle helium-3. *J. Mar. Systems* **48**, 15–36, doi:10.1016/j.jmarsys.2003.05.010 (2004).

12. Prentice, I. C. *et al.* The carbon cycle and atmospheric CO_2. In Houghton, J. T. *et al.* (eds.) *Climate Change 2001: The Scientific Basis, Contribution of Working Group I to the Third Assesment Report of the Intergovernmental Panel on Climate Change*, 183–237 (Cambridge University Press, New York, 2001). Report of the International Panel on Climate Change.

13. Watson, A. J. & Orr, J. C. Carbon dioxide fluxes in the global ocean. In Fasham, M., Field, J., Platt, T. & Zeitzschel, B. (eds.) *Ocean Biogeochemistry: the Role of the Ocean Carbon Cycle in Global Change (a JGOFS Synthesis)*, chap. 5, 123–141 (Springer, Berlin, 2003).

14. Matsumoto, K. *et al.* Evaluation of ocean carbon cycle models with data-based metrics. *Geophys. Res. Lett.* **31**, L07303, doi:10.1029/2003GL018970 (2004).

15. Wright, D. G. & Stocker, T. F. Sensitivities of a zonally averaged global ocean circulation model. *J. Geophys. Res.* **97**, 12707–12730 (1992).

16. Stocker, T. F., Wright, D. G. & Mysak, L. A. A zonally averaged, coupled ocean-atmosphere model for paleoclimate studies. *J. Climate* **5**, 773–797 (1992).

17. Marchal, O., Stocker, T. & Joos, F. A latitude-depth, circulation-biogeochemical ocean model for paleoclimate studies: model development and sensitivities. *Tellus, Ser. B* **50**, 290–316 (1998).

18. Siegenthaler, U. & Oeschger, H. Biospheric CO_2 emissions during the past 200 years reconstructed by deconvolution of ice core data. *Tellus* **39B**, 140–154 (1987).

19. Gordon, H. B. & O'Farrell, S. P. Transient climate change in the CSIRO coupled model with dynamical sea ice. *Mon. Weather Rev.* **125**, 875–907 (1997).

20. Hirst, A., O'Farrell, S. P. & Gordon, H. B. Comparison of a coupled ocean-atmosphere model with and without oceanic eddy-induced advection. Part 1: ocean spinup and control integrations. *J. Clim.* **13**, 139–163 (2000).

21. Matear, R. J. & Hirst, A. C. Climate change feedback on the future oceanic CO_2 uptake. *Tellus* **51B**, 722–733 (1999).

22. Dufresne, J.-L. *et al.* On the magnitude of positive feedback between future climate change and the carbon cycle. *Geophys. Res. Lett.* **29**, 1405, doi:10.1029/2001GL013777 (2002).

23. Joos, F., Plattner, G.-K., Stocker, T. F., Marchal, O. & Schmittner, A. The impact of global warming-marine carbon cycle feedbacks on future atmospheric CO_2. *Science* **284**, 464–467 (1999).

24. Plattner, G.-K., Joos, F., Stocker, T. F. & Marchal, O. Feedback mechanisms and sensitivities of ocean carbon uptake under global warming. *Tellus* **53B**, 564–592 (2001).

25. Madec, G., Delecluse, P., Imbard, M. & Lévy, C. OPA version 8.0, Ocean General Circulation Model, Reference Manual. Note of the IPSL Modelling Pole 11, IPSL (1998).

26. Rodgers, K. B. *et al.* Radiocarbon as a thermocline proxy for the eastern equatorial Pacific. *Geophys. Res. Lett.* **31**, L14314,doi:10.1029/2004GL019764 (2004).

27. Aumont, O., Maier-Reimer, E., Blain, S. & Monfray, P. An ecosystem model of the global ocean including Fe, Si, P colimitations. *Global Biogeochem. Cycles* **17**, 1060, doi:10.1029/2001GB001745 (2003).

28. Bopp, L., Kohfeld, K. E., Quéré, C. L. & Aumont, O. Dust impact on marine biota and atmospheric CO_2 during glacial periods. *Paleoceanography* **18**, 1046, doi:10.1029/2002PA000810 (2003).

29. Feely, R. A. *et al.* Oxygen utilization and organic carbon remineralization in the upper water column of the pacific ocean. *J. Oceanograph.* **60**, 45–52 (2004).

30. Garcia, H. E., Boyer, T. P., Levitus, S., Locarnini, R. A. & Antonov, J. On the variability of dissolved oxygen and apparent oxygen utilization content for the upper world ocean: 1955 to 1998. *Geophys. Res. Lett.* **32**, L09604, doi:10.1029/2004GL022286 (2005).

31. Sarmiento, J. L., Hughes, T. M. C., Stouffer, R. J. & Manabe, S. Simulated response of the ocean carbon cycle to anthropogenic climate warming. *Nature* **393**, 245–249 (1998).

32. Bopp, L. *et al.* Potential impact of climate change of marine export production. *Global Biogeochem. Cycles* **15**, 81–99 (2001).

33. Matear, R. J., Hirst, A. C. & McNeil, B. I. Changes in dissolved oxygen in the southern ocean with climate change. *Geochem. Geophys. Geosyst.* Paper number 2000GC000086 (2000).

34. Matear, R. J. & Hirst, A. C. Long-term changes in dissolved oxygen concentrations in the ocean caused by protracted global warming. *Global Biogeochem. Cycles* **17**, 1125, doi:10.1029/2002GB001997 (2003).

35. Anderson, L. A. & Sarmiento, J. L. Redfield ratios of remineralization determined by nutrient data analysis. *Global Biogeochem. Cycles* **8**, 65–80 (1994).

36. Deutsch, C., Emerson, S. & Thompson, L. Fingerprints of climate change in North Pacific oxygen. *Geophys. Res. Lett.* **in revision** (2005).

37. Emerson, S., Watanabe, Y., Ono, T. & Mecking, S. Temporal trends in apparent oxygen utilization in the upper pycnocline of the North Pacific. *J. Oceanograph.* **60**, 139–147 (2004).

38. Heinze, C. Simulating oceanic $CaCO_3$ export production in the greenhouse. *Geophys. Res. Lett.* **31**, L16308, doi:10.1029/2004GL020613 (2004).

39. Andersson, A. J., Mackenzie, F. T. & Ver, L. M. Solution of shallow-water carbonates: An insignificant buffer against rising atmospheric CO_2. *Geology* **31**, 513–516 (2003).

40. Archer, D., Kheshgi, H. S. & Maier-Reimer, E. Dynamics of fossil fuel CO_2 neutralization by marine $CaCO_3$. *Global Biogeochem. Cycles* **12**, 259–276 (1998).

41. Sarma, V. V. S. S., Ono, T. & Saino, T. Increase of total alkalinity due to shoaling of aragonite saturation horizon in the Pacific and Indian Oceans: Influence of anthropogenic carbon inputs. *Geophys. Res. Lett.* **29**, 1971, doi:10.1029/2002GL015135 (2002).

42. Taylor, K. E. Summarizing multiple aspects of model performance in single diagram. *J. Geophys. Res.* **106**, 7183–7192 (2001).

43. Sabine, C. L. *et al.* The ocean sink for anthropogenic CO_2. *Science* **305**, 367–370 (2004).